ISTITUTO NAZIONALE DI FISICA NUCLEARE
Laboratori Nazionali di Frascati

LNF-80/75

G. Bizard et al. :

EXPERIMENTAL STUDY AND BARYONIC EXCHANGE INTERPRETATION OF THE REACTION $^{2}H(d,n)^{3}He$ IN THE INTERMEDIATE ENERGY REGION

Estratto da :

Phys. Rev. C22, 1632 (1980)

Servizio Documentazione
dei Laboratori Nazionali di Frascati
Cas. Postale 13 - Frascati (Roma)

Experimental study and baryonic exchange interpretation of the reaction $^2H(d,n)^3He$ in the intermediate energy region

G. Bizard, J. L. Laville, C. Le Brun, J. F. Lecolley, F. Lefebvres, A. Osmont, R. Regimbart, and J. C. Steckmeyer
Laboratoire de Physique Corpusculaire LA 34 associé à l'IN2P3, ISMRA, Université de Caen, France

J. Berger, J. Duflo, L. Goldzahl, J. Oostens,* and F. Plouin
Institut National de Physique Nucléaire et de Physique des Particules, Laboratoire National Saturne, Saclay, France

F. L. Fabbri, P. Picozza, and L. Satta
Istituto Nazionale di Fisica Nucleare, Laboratori Nazionali di Frascati, Frascati, Italy

(Received 19 February 1980)

We present a complete set of eight differential cross sections of the reactions $^2H(d,n)^3He$ and $^2H(d,p)^3H$ in the 0–60° c.m. angular range for incident deuteron momenta between 1.1 and 2.5 GeV/c. A simple phenomenological interpretation of the energy dependence of the total cross section σ_T and of $d\sigma/dt$ at fixed t shows, in the reaction, the contribution of a nucleon exchange process to which we must add a mechanism implying the Δ_{33} resonance excitation in the direct channel.

[NUCLEAR REACTION $^2H(d,n)^3He$, $^2H(d,p)^3H$; $E_d = 0.3 - 1.25$ GeV; measured $\sigma(E_d, \theta)$; intermediate energy; phenomenological analysis of the baryonic exchange mechanisms.]

I. INTRODUCTION

The $^2H(d,n)^3He$ reaction belongs to the same class of baryonic-exchange processes as the nucleon-deuteron backward elastic scattering which has been extensively studied in the recent past. The 180° elastic Nd cross sections, extrapolated from the experimental backward peaks[1] are well described at low energy, below $T_N = 300$ MeV by the one-nucleon exchange (ONE) model using the nucleon wave functions of the deuteron. Above 300 MeV, strong deviations of the ONE model from experimental data appear. Several theoretical explanations have been given to understand the rise of the Nd backward differential cross section for energies between 300 and 1500 MeV.

The first one is due to Kerman and Kisslinger[2] who explained the observed backward rise with an additional new mechanism, the N^* exchange in the u channel which is favored for high momentum transfers. This hypothesis of an N^*N component of the order of 1.5% inside the deuteron led to numerous experimental and theoretical investigations on the existence of isobar configurations inside nuclei[3] which did not allow, up to now, definite conclusions.

Another explanation was suggested by Craigie and Wilkin[4] and by Barry[5] to reproduce the pd backward scattering above 300 MeV neglecting ONE. That is, a mechanism implying a one-nucleon exchange followed by a π exchange; let us call this model ONPE. Within this model, the $^2H(p,p)^2H$ scattering can be expressed through the $^1H(p,\pi^+)^2H$ one. The resonant behavior of this last reaction versus the total c.m. energy is well explained by Yao,[6] using a two-step mechanism: first, a virtual π exchange between the two initial nucleons followed by the excitation of a Δ_{33} resonance, and then a nucleon exchange leading to the deuteron formation. Qualitatively, via the $^1H(p,\pi^+)^2H$ reaction, this model sets a link between the $^2H(p,d)^1H$ energy dependence and the excitation function of the Δ_{33} resonance.

A recent complete experimental study[1] of the nd scattering around 180° for energies between 200 and 800 MeV confirms without ambiguity the

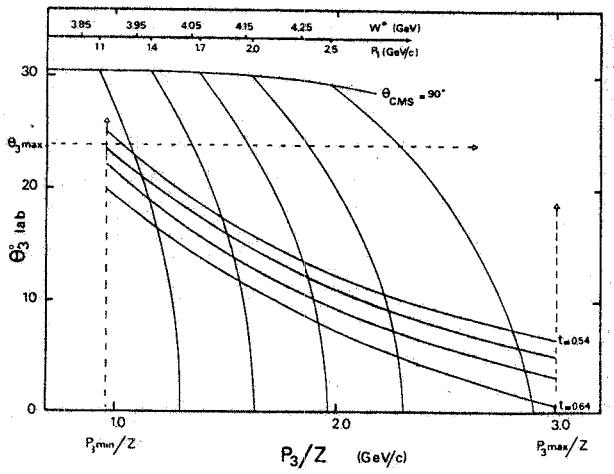

FIG. 1. $^2H(d,n)^3He$ n kinematics for ^3He; laboratory angle θ_3 versus momentum p_3/z for various p_l deuteron incident momenta shown in the upper scale, W^* being the corresponding energy in the c.m.s.

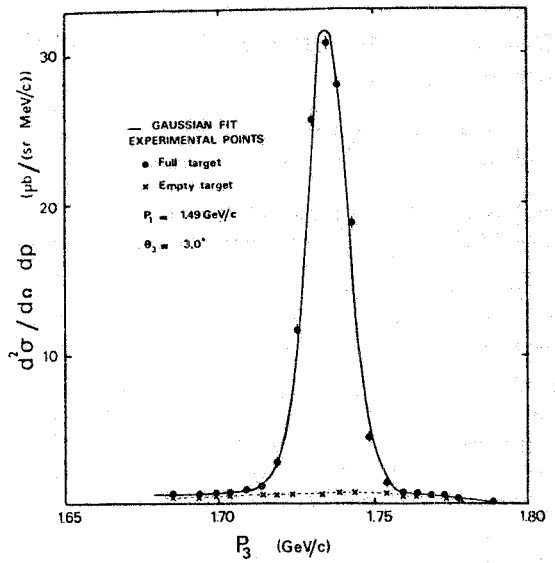

FIG. 2. An experimental momentum spectrum with the empty target contribution of $^2H(d,p)^3H$ reaction.

presence of a plateau around 550 MeV. To this energy is associated an invariant mass very close to the sum of the masses $2m_N + m_{\Delta_{33}}$, which confirms the part played by the excitation of the Δ_{33} resonance in the direct channel. The experimental results[1] are well reproduced by the model of Kolybasov and Smorodinskaya[7] that implies both ONE and ONPE amplitudes. In addition, the first measurement of the analyzing power of the reaction $p+d \to dp$ at 316 and 516 MeV (Ref. 8) confirms the need to take into account above 300 MeV, the N-N rescattering and the ONE along with the ONPE.

As in the $^2H(p,d)^1H$ the $^2H(d,n)^3H$ process implies high momentum transfers and a fixed energy analysis of this reaction would require a good knowledge of the high momentum components of the wave functions of nucleon and possible N^* inside the nuclei. A way to overcome this difficulty is to perform at fixed t (incident deuteron to ^3He four-momentum transfer squared), an energy dependent analysis, in order to be free from the t dependence of relativistic form factors associated with light nucleus formation. With this idea in mind, the energy and angular range of the experiment was determined to fulfill two conditions: a complete exploration of the Δ_{33} excitation domain, and a t overlap as large as possible between the different measurements. In this energy range, the $^2H(d,n)^3He$ reaction had never been measured, the nearest available data being those[9] at 0.564 GeV/c.

II. EXPERIMENT AND RESULTS

In this experiment, we used the Saturne I ex-

TABLE I. Differential cross section of the $^2H(d,p)^3H$ reaction.

P_1=1.109 GeV/c W^*=3.895 GeV		P_1=1.387 GeV/c W^*=3.974 GeV		P_1=1.493 GeV/c W^*=4.003 GeV		P_1=1.651 GeV/c W^*=4.051 GeV		P_1=1.787 GeV/c W^*=4.093 GeV	
t (GeV/c)^2	^3H $\frac{d\sigma}{dt}$ μb/(GeV/c)^2	t (GeV/c)^2	^3H $\frac{d\sigma}{dt}$ μb/(GeV/c)^2	t (GeV/c)^2	^3H $\frac{d\sigma}{dt}$ μb/(GeV/c)^2	t (GeV/c)^2	^3H $\frac{d\sigma}{dt}$ μb/(GeV/c)^2	t (GeV/c)^2	^3H $\frac{d\sigma}{dt}$ μb/(GeV/c)^2
0.806	6330 ± 573	0.769	690 ± 51	0.757	406 ± 29	0.720	221 ± 7	0.699	136 ± 7
0.769	2867 ± 245	0.758	513 ± 43	0.743	301 ± 16	0.695	132.5 ± 4.7	0.671	111 ± 7
0.785	1655 ± 201	0.738	339 ± 18	0.721	214 ± 9.3	0.660	89.2 ± 2.9	0.630	69.6 ± 4.2
0.759	826 ± 76	0.714	228 ± 22	0.694	157 ± 12	0.621	44.9 ± 1.4	0.581	25.4 ± 2.3
0.746	656 ± 38	0.647	77.3 ± 3.3	0.658	83.4 ± 3.5	0.568	19.2 ± 0.8	0.527	10.4 ± 0.5
0.727	492 ± 33	0.495	18.0 ± 0.9	0.616	43.4 ± 1.7	0.510	8.23 ± 0.40		
0.696	343 ± 16	0.431	15.2 ± 0.7	0.565	20.9 ± 0.7	0.438	5.50 ± 0.32		
0.665	236 ± 14	0.355	13.2 ± 0.7	0.506	12.2 ± 0.4	0.357	4.81 ± 0.27		
0.630	158 ± 9	0.715	230 ± 22	0.439	9.7 ± 0.4	0.268	5.04 ± 0.25		
0.589	114 ± 5	0.686	142 ± 7	0.366	9.4 ± 0.4	0.164	4.33 ± 0.25		
0.541	88 ± 3	0.648	79.3 ± 4.6	0.282	8.3 ± 0.3				
		0.602	42.1 ± 4.1						
		0.552	23.8 ± 2.0						
		0.499	17.3 ± 0.7						

TABLE II. Differential cross section of the $^2H(d,n)^3He$ reaction.

$P_1=1.651$ GeV/c $W^*=4.093$ GeV ^{3}He		$P_1=1.89$ GeV/c $W^*=4.127$ GeV ^{3}He		$P_1=1.992$ GeV/c $W^*=4.159$ GeV ^{3}He		$P_1=2.492$ GeV/c $W^*=4.329$ GeV ^{3}He	
t (GeV/c)^2	$\frac{d\sigma}{dt}$ μb/(GeV/c)	t (GeV/c)^2	$\frac{d\sigma}{dt}$ μb/(GeV/c)	t (GeV/c)^2	$\frac{d\sigma}{dt}$ μb/(GeV/c)	t (GeV/c)^2	$\frac{d\sigma}{dt}$ μb/(GeV/c)
0.742	293.3 ± 7.8	0.711	147 ± 10.4	0.700	116.1 ± 7	0.643	29.0 ± 2.1
0.735	246.8 ± 6.9	0.710	141.5 ± 7.5	0.698	100.6 ± 6	0.629	30.0 ± 3.1
0.718	199.7 ± 5.3	0.687	116.9 ± 5.5	0.672	83.0 ± 5.4	0.618	22.5 ± 1.5
0.653	83.9 ± 2.6	0.652	73.1 ± 4.6	0.633	49.5 ± 4.5	0.599	19.5 ± 2.1
0.558	17.84 ± 0.63	0.609	37.9 ± 1.6	0.588	26.4 ± 1.5	0.543	10.5 ± 1.2
0.493	6.55 ± 0.28	0.552	14.95 ± 0.70	0.524	9.82 ± 0.51	0.469	3.83 ± 0.20
0.419	5.12 ± 0.28	0.482	5.48 ± 0.20	0.439	2.80 ± 0.22	0.372	0.972 ± 0.066
0.245	4.81 ± 0.26	0.400	2.38 ± 0.13	0.359	1.64 ± 0.11	0.255	0.482 ± 0.032
		0.303	1.97 ± 0.09	0.252	1.49 ± 0.11	−0.31	0.360 ± 0.030
		0.140	2.18 ± 0.10	0.141	1.47 ± 0.08	−0.401	0.244 ± 0.025
		0.023	2.00 ± 0.09	0.007	1.44 ± 0.08		

tracted deuteron beam of typical intensity 2×10^{11} d/burst with the achromatic double focusing spectrometer and experimental layout described in detail elsewhere.[10,11] In order to minimize the spectrometer reduced acceptance $(\Delta p/p)\Delta\Omega$ variations due to multiple scattering, we measured the reaction $^2H(d,n)^3He$ in the upper incident momentum interval 1.65–2.5 GeV/c and the reaction $^2H(d,p)^3H$ in the lower band 1.1–1.9 GeV/c. An overlap between these two studies was made at 1.65 GeV/c. The particles were identified by their time of flight and energy loss in scintillation counters. At each incident energy, absolute flux calibration was obtained by irradiation of graphite discs. In the deuteron momentum range of this study, a special experiment was made to measure the $^{12}C(d,X)^{11}C$ cross section[12] and we have used the results to obtain an absolute calibration better than ±7%.

For this study, the laboratory angular range was 0° to 24°. Within these experimental boundaries one sees from Fig. 1 that the common t domain is defined by the following limits: $t_1=0.64$ and $t_2=0.54$ (GeV/c)^2. Figure 2 shows a typical experimental peak with the empty target contribution which is always less than 2% in this experiment. All the data listed in Tables I and II were corrected from the losses due to nuclear absorption (always less than 10%). The errors do not include the 10% scale factor due to the uncertainty in the determination of the absolute beam intensity and of the spectrometer acceptance.

The set of our eight differential cross sections is displayed in Fig. 3 versus $t-t_{max}$ with the incident deuteron momentum as a parameter. We verified inside experimental errors, on the 1.65

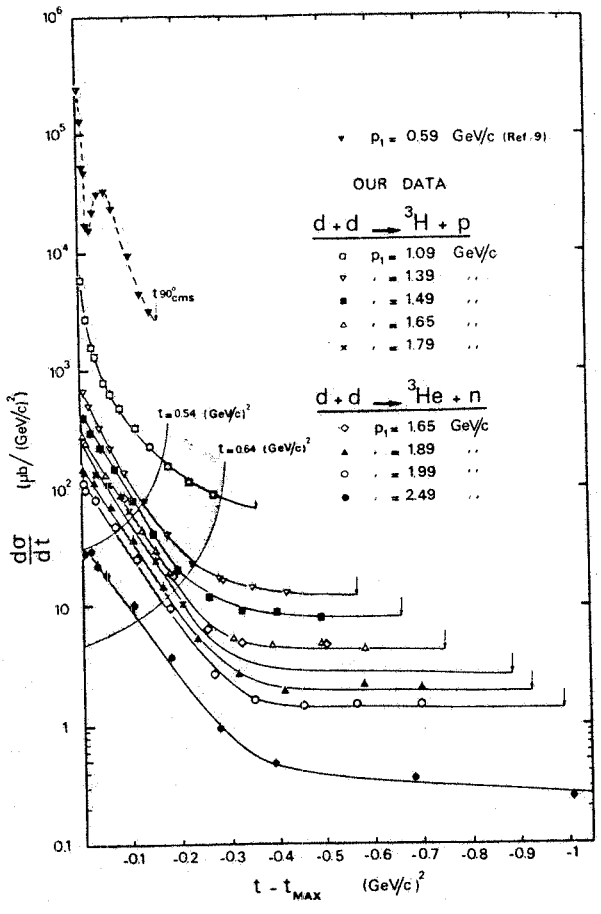

FIG. 3. Our eight differential cross sections versus $t-t_{max}$. In parameter p_1, the deuteron incident momentum. The continuous lines correspond to the fits of formula (1). The shaded area defines the common t domain. Black triangles (▼) are the data of Ref. 9.

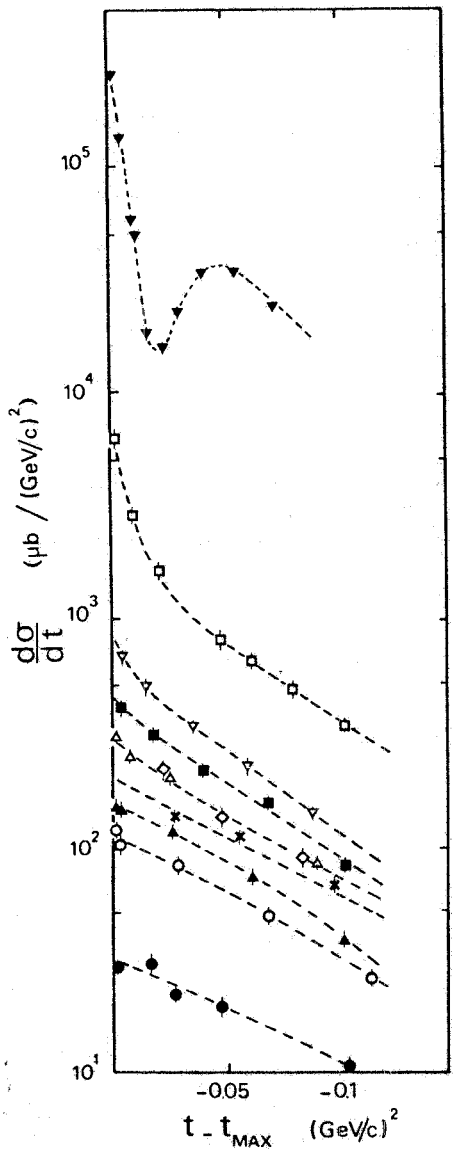

FIG. 4. A forward blowup of the differential cross sections versus $t-t_{max}$.

GeV/c differential cross section, the agreement of the ^{3}He and ^{3}H measurements. The differential cross sections are rapidly decreasing with $t-t_{max}$ and are very different in shape from the 0.564 GeV/c data[9]: no dip is found and the steep forward slope has disappeared except in the lowest energy measurement (Fig. 4). The flattening of the distribution at large $|t|$ is related to the rise of the ^{3}He-d overlap wave function.[13] These results are similar to the ones observed in the ^{4}He$(p,d)^3$He reaction.[14-16] The steep forward slope observed[14] at $T_p=156$ MeV disappears in the higher energy measurements[15,16] where a break in slope is found around the same t value of 0.5 (GeV/c)^2 (four-momentum transfer squared from the incident proton to the final deuteron).

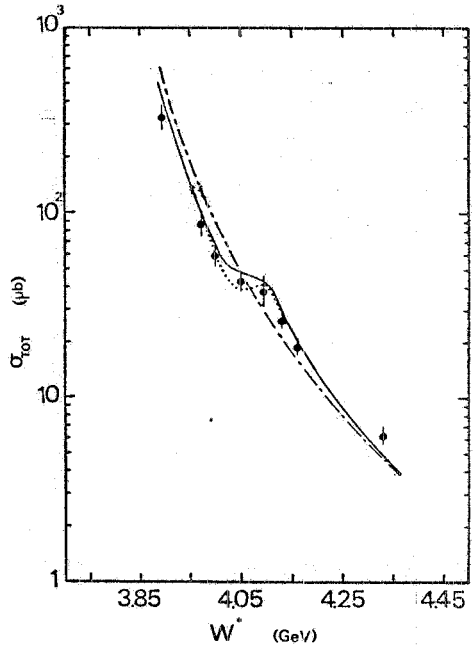

FIG. 5. ^{2}H$(d,n)^3$He, σ_T total cross section versus the total c.m. energy W^*. Continuous curve deduced from formula (2); dash-dotted curve: ONE contribution; dotted curve: ONE contribution plus its interference term with the Breit-Wigner amplitude.

At each incident energy, we fitted our data with the following empirical parametrization:

$$\frac{d\sigma}{dt}=\sum_{i=1}^{3}\alpha_i e^{-\beta_i t}. \tag{1}$$

These parametrizations extrapolated up to a center of mass angle of 90°, and the symmetry property of the ^{3}H$(d,n)^3$He reaction, enable us to calculate the total cross section σ_T of this reaction as a function of the total energy W^* in the c.m. system. The experimental values of σ_T (Fig. 5) show some indication for a shoulder around $W^*=4.05$ GeV corresponding to the sum of the masses $3m_N+m_{\Delta_{33}}$.

III. PHENOMENOLOGICAL ANALYSIS

By analogy with the model[7] that gives a good description of the recent ^{2}H$(n,d)n$ data[1] in terms of ONE and ONPE amplitudes, we analyzed our experimental results with a simple phenomenological model which assumes, in the energy range of this experiment, the dominant contribution of the two graphs shown in Fig. 6. For the ONE amplitude, we used the simple formula $F_N(s,t)=Ae^{\alpha t}/(m_N^2-t)$, where A is a real constant and $e^{\alpha t}$ is an exponential parametrization of the form factors associated to the upper and lower vertices, $s=W^{*2}$ being the

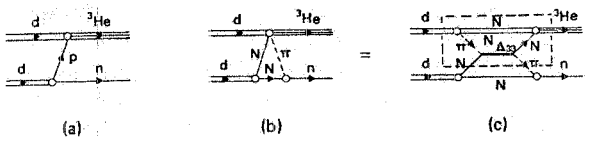

FIG. 6. (a) ONE graph, (b) ONPE graph, (c) In the square box a possible microscopic representation of the upper vertex of (b).

total c.m. energy squared.

Keeping in mind the explanation used for the resonant behavior of the reaction $^1\mathrm{H}(p,\pi^+)^2\mathrm{H}$ by πN scattering, the upper vertex of Fig. 6(b) ($dN \to {}^3\mathrm{He}\pi$) can be represented by the square box of Fig. 6(c). This last graph explains the baryonic exchange mechanism by an intermediate πN interaction leading to Δ_{33} resonance excitation followed by nucleon pickup. The simple parametrization chosen to calculate the contribution of this graph is a relativistic Breit-Wigner amplitude of the form: $F_{\mathrm{BW}}(s,t) = Be^{\beta t}/(s - s_0 - i\Gamma\sqrt{s})$, where B is a real constant, s_0 and Γ are, respectively, the central value in s and the width of the resonance. The factor $e^{\beta t}$ takes into account all the nuclear form factors of Fig. 6(c) and the t dependence of the exchanged nucleon and π. We used the whole set of our 8 differential cross sections in t range 0.54–0.64 $(\mathrm{GeV}/c)^2$ to determine with a χ^2 minimization program the 7 parameters A, B, α, β, s_0, Γ, and n of the following formula:

$$\frac{d\sigma^{th}}{dt} = \frac{1}{sp_i^{*2}} \frac{1}{p_1^n} |F(s,t) + F(s,u)|^2 \qquad (2)$$

with $F(s,t) = F_N(s,t) + F_{\mathrm{BW}}(s,t)$, $1/sp_i^{*2}$ corresponds to the usual two body phase space kinematical factor and $1/p_1^n$ is a phenomenological factor associated to a common energy dependence of F_N and F_{BW} (p_i^*, p_1 being the initial momentum, respectively, in the c.m. and laboratory system). The symmetrization in t and u is required by the initial state of the reaction $^2\mathrm{H}(d,n)^3\mathrm{He}$. To obtain an energy dependent set of $d\sigma/dt$ data at fixed t, we interpolated between our experimental points, using the fits obtained with formula (1). The results of this procedure are shown in Fig. 7. We notice the existence of an oscillation centered around 4.05 GeV. Experimentally, this oscillation decreases very rapidly with t. Here again, the structure appears around the sum of the masses $3m_N + m_{\Delta_{33}}$. The continuous curves on Fig. 7 are the representation of formula (2) with the fitted parameters precedently defined. The numerical value of these parameters are given in the figure captions, but notice here that s_0 and Γ are in agreement with the energy and width of the Δ_{33} resonance. Except for the lower energy, we observe a very good

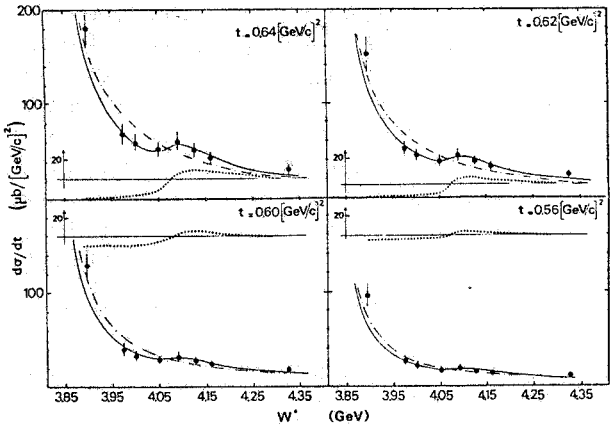

FIG. 7. For 4 fixed t values: 0.64, 0.62, 0.6, and 0.56 $(\mathrm{GeV}/c)^2$, the variations of $d\sigma/dt$ versus W^*, the total energy in the c.m.s. system of the reaction $^2\mathrm{H}(d,n)^3\mathrm{He}$. Continuous curve deduced from formula (2); dash-dotted curve: ONE contribution; dotted-curve: interference term of the ONE contribution with the Breit-Wigner amplitude. Interpolated points are from experimental measurements. Also shown are the different phenomenological contributions of formula (2) with the following fitted parameters: $A = 0.95 \pm 0.02$, $B = (0.92 \pm 0.16)10^{-3}$, $\alpha = 2.93 \pm 0.1$ $(\mathrm{GeV}/c)^{-2}$, $\beta = 12.5 \pm 1.2$ $(\mathrm{GeV}/c)^{-2}$, $s_0 = 16.63 \pm 0.16$ $(\mathrm{GeV})^2$, $(W_0^* = 4.078 \pm 0.020$ GeV), $n = 0.16 \pm 0.05$, $\Gamma = 107 \pm 28$ MeV.

agreement between the experimental points and this simple phenomenological parametrization of the amplitudes associated with Figs. 6(a) and 6(c). The dash-dotted curves represent the only contribution of ONE amplitude. In fact, if we take into account that F_N is real and that, in module, the F_{BW} amplitude is small, the oscillation essentially comes from the interference term (dotted curves); the latter term is only the product of F_N by the real part of F_{BW} which vanishes for the value $s_0 = W_0^2$ of the resonance. We used formula (2) with the fitted parameters to calculate by integration over the whole t range the value of σ_T given by our model, though this expression has only been fitted in the common t region of the data. In Fig. 5, the dash-dotted curve presents the ONE contribution alone that reproduces correctly the general behavior of the results; in the dotted curve, we add the interference contribution, and finally the continuous curve, which contains all the contributions of formula (2), gives a good description of the data.

IV. CONCLUSION

In the intermediate energy range of this experiment, the interaction $^2\mathrm{H}(d,n)^3\mathrm{He}$ is a new tool to study the baryonic exchange mechanisms in reactions between light nuclei. From this simple

phenomenological model, we can conclude that it is necessary to add to the ONE a contribution which involves the nucleon exchange via the excitation of Δ_{33} resonance in the direct channel. This additional mechanism can be reasonably described by Fig. 6(c). Within this phenomenological interpretation no need appears of a contribution coming from an N^* exchange in the t channel. This study confirms the close link between the elementary particle physics and the formation mechanisms of light nucleus via πN scattering. A microscopic calculation[13] of Figs. 6(a) and 6(c) is now in progress and will be published later. As in the case of the pd backward peak, a measurement of the analyzing power in the reaction $^2H(d,n)^3He$ with vector polarized deuterons should permit a better understanding of baryonic exchange mechanisms in this reaction at intermediate energy.

---

*Present address: Physics Department, UCLA, Los Angeles, Calif. 90024.

[1]B. E. Bonner *et al.*, Phys. Rev. Lett. 39, 1253 (1978). This reference contains a complete bibliography on the $Nd \rightarrow dN$ experimental results.
[2]A. K. Kerman and L. S. Kisslinger, Phys. Rev. 180, 1483 (1969).
[3]H. J. Weber and H. Arenhovel, Phys. Rep. 36C, 4 (1978).
[4]N. S. Craigie and C. Wilkin, Nucl. Phys. B14, 477 (1969); C. Wilkin, J. Phys. G (to be published).
[5]G. W. Barry, Ann. Phys. (N.Y.) 73, 482 (1972); Phys. Rev. D 7, 1441 (1973).
[6]T. Yao, Phys. Rev. 134, 454 (1964).
[7]V. M. Kolybasov and N. Y. A. Smorodinskaya, Yad. Fiz. 17, 1211 (1973) [Sov. J. Nucl. Phys. 17, 630 (1973)].
[8]A. N. Anderson *et al.*, Phys. Rev. Lett. 40, 1553 (1978).
[9]M. Roy *et al.*, Phys. Lett. 29B, 2 (1969).
[10]J. Berger *et al.*, Phys. Lett. 63B, 111 (1976).
[11]G. Bizard *et al.*, Nucl. Phys. A267, 503 (1976).
[12]H. Quechon *et al.* (unpublished).
[13]J. M. Laget, J. F. Lecolley, and F. Lefebvres (unpublished).
[14]M. Bernas *et al.*, Nucl. Phys. A156, 289 (1970).
[15]J. Berger *et al.*, Nuovo Cimento Lett. 19, 287 (1977).
[16]T. Bauer *et al.*, Phys. Lett. 67B, 265 (1977).